Analytical model of magnetically actuated mucociliary pumping in a bronchial tube

S Shaheen[1], K Maqbool[1] and A M Siddiqui[2]

[1] Department of Mathematics & Statistics, International Islamic University, Islamabad 44000, Pakistan
[2] Department of Mathematics, York Campus, Pennsylvania State University, 1031 Edgecomb Avenue York, PA 17403, United States of America

E-mail: khadija.maqbool@iiu.edu.pk

Abstract
In this study we investigate the concept of magnetically actuated mucociliary pumping in a bronchial tube. To analyze the muco ciliary clearance in bronchial tube different techniques have been used to observe the ciliary beat frequency. CT-scan and MRI-scan are very effective to detect the ciliary motions which are possible due to the presence of magnetic field. In this study velocity, pressure difference and flow rate are analyzed with the help of continuity equation, Darcy's law and non-linear momentum equation. The mucus layer is considered as a viscoelastic fluid, therefore stress components are simplified for the Maxwell fluid (viscoelastic model). The transportation of mucus layer in the bronchial tube with the help of ciliary movement is modeled in the wave and fixed frame. The resulting PDE's are solved by the perturbation and Adomian decomposition method. Effects of magnetic field, Darcy's resistance and viscoelastic parameter are discussed at length in the graphical results section.

Keywords: strong viscous forces, constant magnetic field, Darcy's law, ciliated bronchial tube, mucociliary clearance

(Some figures may appear in colour only in the online journal)

Nomenclature

Symbol	Description
V	velocity field
W, U	axial and radial velocity in fixed frame
J	current density
B_0	strength of constant magnetic field
R	Darcy's resistance
P	pressure
ψ	stream function
S	stress tensor
c	wave speed
k	permeability of porous medium
M	Hartmann number
a	mean radius of tube
λ	wavelength
ε	cilia length
α	eccentricity of elliptical path
σ	electrical conductivity
β	wave number
λ_1	relaxation time
D_a	Darcy's number

1. Introduction

Biofluid mechanics have become an important subject in the medical field. It produces a nice view of physical phenomena occurring in the body without any surgery. Many organs such as kidney and heart have already discussed by different scientists using mathematical model [1, 2]. A bronchial tube is about 1.09 cm long and having radius 1.5 mm in human body. Human inhale oxygen (air) in the respiratory system through trachea with all pollutants and dirt. In healthy

bronchial tube most of the tube is filled with air but we have considered the case of diseased bronchial tube. A disease 'Bronchitis' is caused by inflammation of airways and in response to these inflammations goblet cells present in epithelial tissues produces excess amount of mucus in bronchial tube. Thus most of the bronchial tube is filled with mucus and cilia helps to transport mucus out of bronchial tube through coughing and sneezing. The respiratory system cleans the mucus from dirt with the help of cilia. Cilia are hair like structure present in the epithelial tissues of respiratory tract. The ciliary movement helps to expel the dirt and pollutants from the mucus present in our body which is known as muco ciliary clearance. Since the human organs like heart, lungs, trachea and tissues are not solid therefore these organs have small pores and the fluid flow through these organs like bronchial tube requires the Darcy's law. The mathematical model of magnetically actuated muco ciliary pumping in bronchial tube is presented with the help of law of conservation of momentum and Darcy's law under the effect of constant magnetic field.

Transportation of fluids under the action of ciliary motion is one of the basic problems in biomedical sciences. Cilia and flagella oscillate in a waving fashion to transport fluids and propel cells. Cilia motion contributes a pivotal role in physiological processes of alimentation, circulation, locomotion, respiration and reproduction [3–5]. The cycle of beat of single cilium separated into effective and recovery stroke. Fluid can flow very rapidly during effective stroke because of large curvature at the base of cilium [6–9]. The hydrodynamic coupling encourages adjacent cilia to beat with a constant phase difference to one another. A field or row of cilia beating in this manner is said to be metachronism. This combined movement of cilia has been used in many biological and psychological studies [8, 10].

In this paper we are interested to investigate the role of cilia for the movement of mucus in the bronchial tube. The moving cilia which are responsible for muco ciliary clearance have the metachronal wave pattern. It is also mentioned in literature [11, 12] that all ciliary activity taking place due to hydrodynamic interactions among the cilia and their surrounding cells and bio fluids. Some important and recent detailed works on hydrodynamics interactions may be credited to Dauptain [13] and Guo [14].

It is evident that microorganisms when causes infection in human body, can die with the application of constant magnetic field strength. It is observed by the medical doctors that tuberculosis skin lesion is completely recovered by the antibiotic having constant negative strength of magnetic field. It is also observed by the physicians that for throat infection when pulmonary cilia are not working properly antibiotics containing magnetic field help to die out the virus that effects the pulmonary cilia movement. The magnetic field acting on the cilia lead to a reduction of the asymmetric area for the case of symplectic metachrony compared to antiplectic metachrony also external magnetic field increase the ciliary beat frequency due to which cilia requires less energy (ATP) to beat. Recently several researchers [15–19] introduced the

study of ciliary and peristaltic motion where they used the magnetic field to observe the wave frequency.

Keeping in view the importance of ciliary movement and Maxwell fluid model with reference to MCC (muco ciliary clearance). In this study we have considered the mathematical model of magnetically actuated muco ciliary pumping in bronchial tube with Darcy's law and constant magnetic field. The governing partial differential equations are simplified by stream function. The effects of inertial forces appearing in governing equations of magnetically actuated muco ciliary pumping in bronchial tube are modeled and solved by perturbation method and Adomian decomposition method (ADM). The graphical results are included for the pressure rise, pressure gradient and velocity distribution.

2. Mathematical model

For the muco ciliary pumping in the bronchial tube, we have considered a ciliated symmetric tube of finite length l with radius a, which is resembling with a bronchial tube having epithelial tissues. The mucus layer in the respiratory tract is a viscoelastic fluid which is resembling with the Maxwell fluid possessing both viscous and elastic properties which is shown in Figure 1. In this study we have used the envelope model [20, 21] approach for the magnetically actuated muco ciliary pumping in the bronchial tube.

In an axisymmetric tube the cilia tips moving in elliptical path therefore position of fluid particles is defined by the following expression
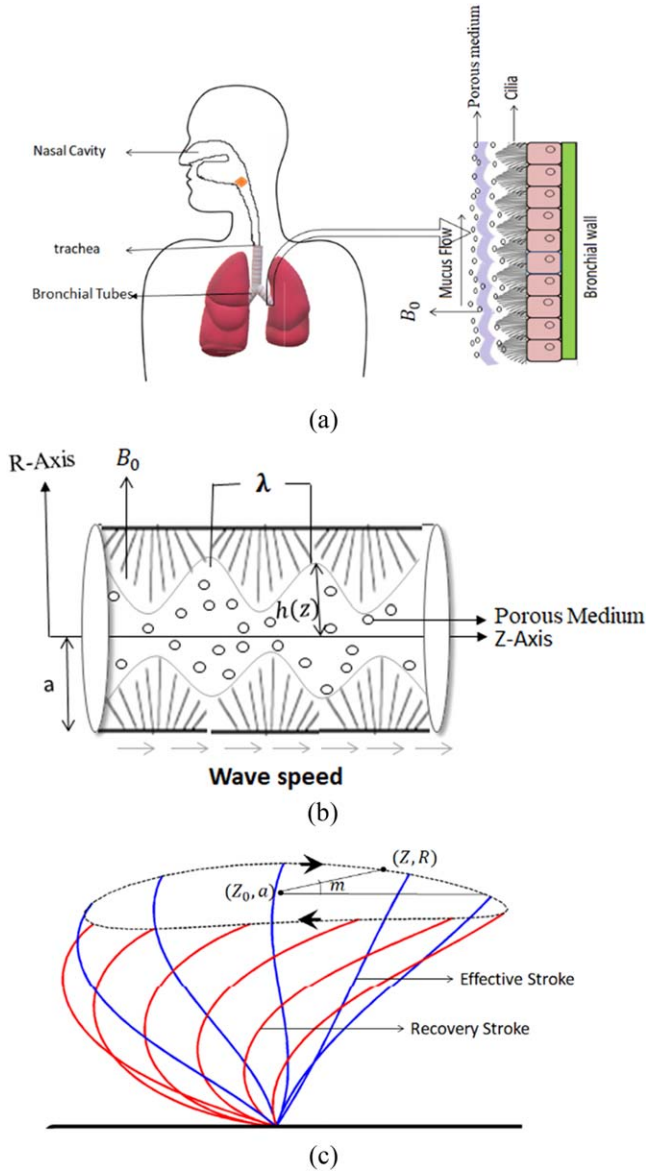
$$R^* = f(Z^*, t^*) = a + a\varepsilon \cos m \qquad (1)$$

$$Z^* = g(Z^*, Z_0^*, t^*) = Z_0^* + a\varepsilon\alpha \sin m, \qquad (2)$$

where $m = \frac{2\pi}{\lambda}(Z^* - ct^*)$, a, ε, Z_0^*, α, λ and c represents mean radius of tube, cilia length parameter, reference position of cilia, eccentricity of ellipse, wavelength and wave speed of metachronal wave respectively. According to no slip condition of velocity R^* and Z^* components of velocity are given as follows

$$U^* = \frac{\partial R^*}{\partial t^*}\bigg|_{Z^* = Z_0^*} = \frac{\partial f}{\partial t^*} + \frac{\partial f}{\partial Z^*}\frac{\partial Z^*}{\partial t^*} = \frac{\partial f}{\partial t^*}$$
$$+ \frac{\partial f}{\partial Z^*}W^*, \qquad (3)$$

$$W^* = \frac{\partial Z^*}{\partial t^*}\bigg|_{Z^* = Z_0^*} = \frac{\partial g}{\partial t^*} + \frac{\partial g}{\partial Z^*}\frac{\partial Z^*}{\partial t^*} = \frac{\partial g}{\partial t^*}$$
$$+ \frac{\partial g}{\partial Z^*}W^*, \qquad (4)$$

Figure 1. (a) Geometry of bronchial tube. (b) Geometry of diseased bronchial tube. (c) Formation of elliptic wave.

Substituting equations (1), (2) in (3)), we get

$$W^* = \frac{-\left(\frac{2\pi}{\lambda}\right)[\varepsilon a \alpha c \cos m]}{1 - \left(\frac{2\pi}{\lambda}\right)[\varepsilon a \alpha c \cos m]} \quad (5)$$

and

$$U^* = \frac{\left(\frac{2\pi}{\lambda}\right)[\varepsilon a \alpha c \sin m]}{1 - \left(\frac{2\pi}{\lambda}\right)[\varepsilon a \alpha c \cos m]}. \quad (6)$$

The wave frame and fixed frame are related by the following transformation

$$z^* = Z^* - ct^*, r^* = R^*, w^* = W^* - c, u^*$$
$$= U^*, p^*(z, r) = P^*(Z, R, T), \quad (7)$$

where r^*, z^*, w^*, u^* and p^* are the quantities in wave frame and R^*, Z^*, W^*, U^* and P^* are in fixed frame.

For the magnetically actuated muco ciliary pumping in the bronchial tube following velocity profile is appropriate along the axis and radius of tube (bronchial tube)

$$\boldsymbol{V} = [u(r, z), 0, w(r, z)]. \quad (8)$$

For the transportation of mucus layer through the bronchial tube, the continuity equation and momentum equation with Darcy's law in the presence of magnetic field [22] are expressed as follows

$$\nabla . \boldsymbol{V} = 0, \quad (9)$$

and

$$\rho \frac{d\boldsymbol{V}}{dt} = \text{div } \boldsymbol{T} + \boldsymbol{F}, \quad (10)$$

where

$$\boldsymbol{F} = \boldsymbol{J} \times \boldsymbol{B} + \boldsymbol{R}, \quad (11)$$

and

$$\boldsymbol{J} \times \boldsymbol{B} = -\sigma B_0^2 (w + c) \quad (12)$$

$$\boldsymbol{T} = -p\boldsymbol{I} + \boldsymbol{S}, \quad (13)$$

$$\boldsymbol{S} + \lambda_1 \left(\frac{d\boldsymbol{S}}{dt} - \boldsymbol{LS} - \boldsymbol{SL}^T \right) = \mu \boldsymbol{A}_1. \quad (14)$$

In above equations $\boldsymbol{V}$ represents the velocity field, T the extra stress tensor, $\boldsymbol{S}$ the Cauchy stress tensor, ρ the density of fluid, $\boldsymbol{J}$ the current density, B_0 the strength of applied magnetic field, σ the electrical conductivity of the fluid, $\boldsymbol{R}$ the Darcy's resistance, L gradient of velocity, p the pressure, μ the viscosity of fluid, λ_1 the relaxation time of Maxwell fluid and $\boldsymbol{A}_1$ the first Rivilian Erickson tensor.

In the muco ciliary pumping, the velocity, pressure and shear stress need to be analyzed, therefore continuity and momentum equation together with the stress and strain relationship are expressed in the following manner

$$\frac{1}{r} \frac{\partial}{\partial r}(ru) = -\frac{\partial w}{\partial z}, \quad (15)$$

$$\rho \left(u \frac{\partial u}{\partial r} + w \frac{\partial u}{\partial z} \right) = -\frac{\partial p}{\partial r} + \frac{1}{r} \frac{\partial}{\partial r}(rS_{rr}) + \frac{\partial S_{rz}}{\partial z}$$
$$- \frac{S_{\theta\theta}}{r} - \frac{\mu}{\kappa} u, \quad (16)$$

$$\rho \left(u \frac{\partial w}{\partial r} + w \frac{\partial w}{\partial z} \right) = -\frac{\partial p}{\partial z} + \frac{1}{r} \frac{\partial}{\partial r}(rS_{zr}) + \frac{\partial S_{zz}}{\partial z}$$
$$- \sigma B_0^2 w - \frac{\mu}{\kappa} w, \quad (17)$$

where shear and normal stresses satisfying the following expressions
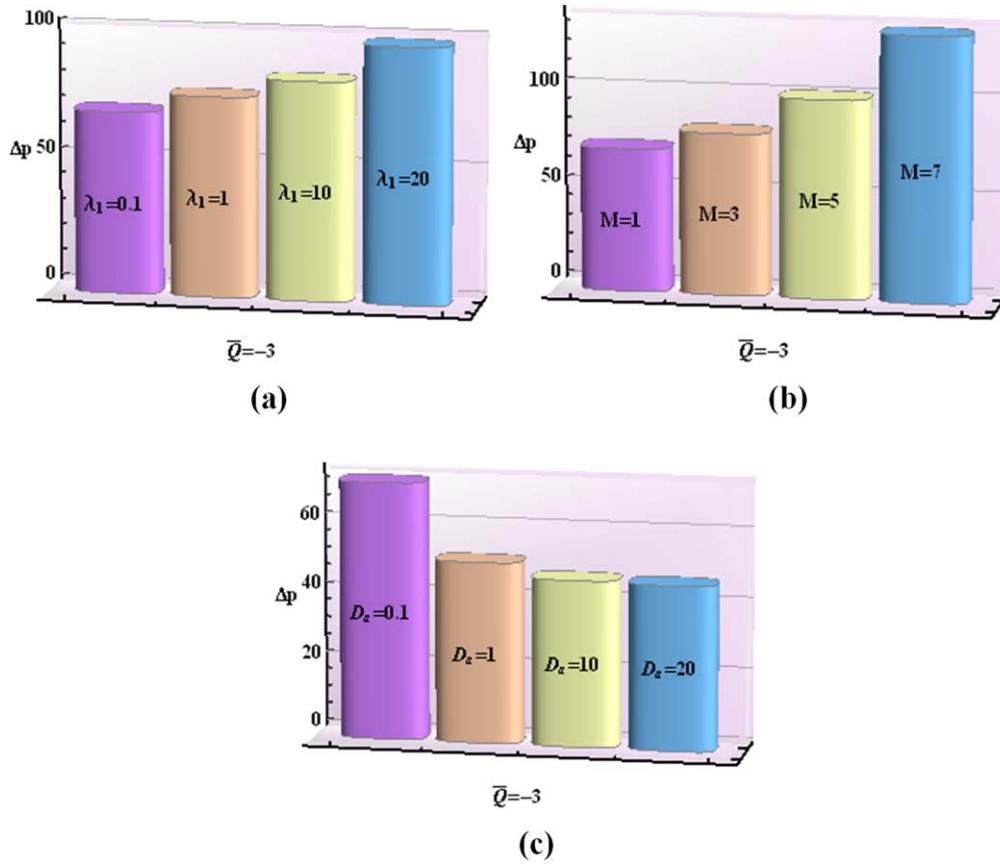
Figure 2. (a)–(c) Barchart of pressure rise for distinct values of λ_1, M, D_a. When $Re = 1$, $\beta = 0.1$, $\alpha = 0.4$, $r = 0.3$ and $\varepsilon = 0.2$ are kept fixed.

$$S_{rr} + \lambda_1 \left(u\frac{\partial S_{rr}}{\partial r} + w\frac{\partial S_{rr}}{\partial z} - 2\frac{\partial u}{\partial r}S_{rr} - 2\frac{\partial u}{\partial z}S_{rz} \right)$$
$$= 2\mu\frac{\partial u}{\partial r}, \tag{18}$$

$$S_{r\theta} + \lambda_1 \left(u\frac{\partial S_{r\theta}}{\partial r} + w\frac{\partial S_{r\theta}}{\partial z} - \frac{\partial u}{\partial r}S_{r\theta} - \frac{\partial u}{\partial z}S_{z\theta} \right.$$
$$\left. - \frac{u}{r}S_{r\theta} \right) = 0 \tag{19}$$

$$S_{rz} + \lambda_1 \left(u\frac{\partial S_{rz}}{\partial r} + w\frac{\partial S_{rz}}{\partial z} - \left(\frac{\partial w}{\partial z} + \frac{\partial u}{\partial r} \right)S_{zr} \right.$$
$$\left. - \frac{\partial u}{\partial z}S_{zz} - \frac{\partial w}{\partial r}S_{rr} \right) = \mu\left(\frac{\partial u}{\partial z} + \frac{\partial w}{\partial r} \right), \tag{20}$$

$$S_{\theta\theta} + \lambda_1 \left(u\frac{\partial S_{\theta\theta}}{\partial r} + w\frac{\partial S_{\theta\theta}}{\partial z} - 2\frac{u}{r}S_{\theta\theta} \right) = 2\mu\frac{u}{r}, \tag{21}$$

$$S_{\theta z} + \lambda_1 \left(u\frac{\partial S_{\theta z}}{\partial r} + w\frac{\partial S_{\theta z}}{\partial z} - \left(\frac{uS_{\theta z}}{r} + \frac{\partial w}{\partial z}S_{\theta z} \right) \right.$$
$$\left. - \frac{\partial w}{\partial r}S_{r\theta} \right) = 0 \tag{22}$$

$$S_{zz} + \lambda_1 \left(u\frac{\partial S_{zz}}{\partial r} + w\frac{\partial S_{zz}}{\partial z} - 2\frac{\partial w}{\partial r}S_{rz} - 2\frac{\partial w}{\partial z}S_{zz} \right)$$
$$= 2\mu\frac{\partial w}{\partial z}. \tag{23}$$

The mucus layer covers the region $-h \leqslant r \leqslant h$ and $-l/2 \leqslant z \leqslant l/2$ where the no slip condition requires that velocity of the cilia tips and fluid adjacent to the cilia tips are same, therefore the following boundary conditions on the cilia tips are defined as follows

$$w = w(h) = \frac{-\left(\frac{2\pi}{\lambda}\right)[\varepsilon a\alpha c \sin n]}{1 - \left(\frac{2\pi}{\lambda}\right)[\varepsilon a\alpha \cos n]} \tag{24a}$$
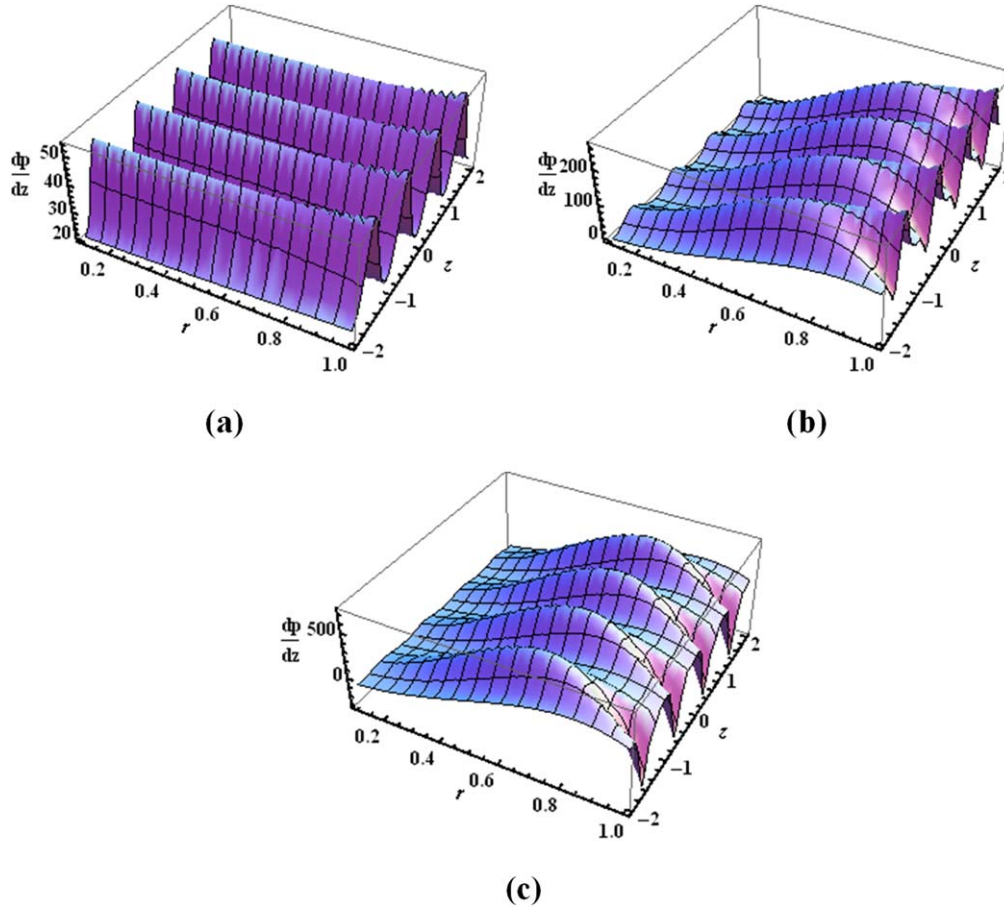
$$u = u(h) = \frac{\left(\frac{2\pi}{\lambda}\right)[\varepsilon a\alpha c \sin n]}{1 - \left(\frac{2\pi}{\lambda}\right)[\varepsilon a\alpha \cos n]} \tag{24b}$$

at

$$r = \pm h(z) = \pm[a + \varepsilon\alpha a \cos n], \tag{24c}$$

where

$$n = \frac{2\pi}{\lambda}z.$$

Figure 3. (a)–(c) 3D view of pressure gradient for $M = 1,\ 5,\ 10$. When $Re = 1, \beta = 0.1, \alpha = 0.4, \varepsilon = 0.2, D_a = 1, \lambda_1 = 0.1$ and $\bar{Q} = -3$ are kept fixed.

The biological flows are poiseuille type which requires that flow is maximum at the centre line of the ciliated tube, therefore axial velocity at $r = 0$ (centre line) satisfies the following condition

$$\frac{\partial w}{\partial r} = 0 \text{ at } r = 0. \tag{25}$$

For the mathematical computation following non-dimensional quantities are require

$$z^* = \frac{z}{\lambda},\ r^* = \frac{r}{a},\ u^* = \frac{u}{\beta c},\ w^* = \frac{w}{c},\ h^* = \frac{h}{a},$$

$$p^* = \frac{a\beta}{c\mu}p,\ \beta = \frac{a}{\lambda},\ S_{ij}^* = \frac{a}{\mu c}S_{ij},\ \lambda_1^* = \frac{c\lambda_1}{a},$$

$$Re = \frac{\rho ac}{\mu},\ M = \sqrt{\frac{\sigma}{\mu}}aB_0^2,\ D_a = \frac{k}{a^2}. \tag{26}$$

After dropping '*' non-dimensional form of equations (15)–(25) are given as follows
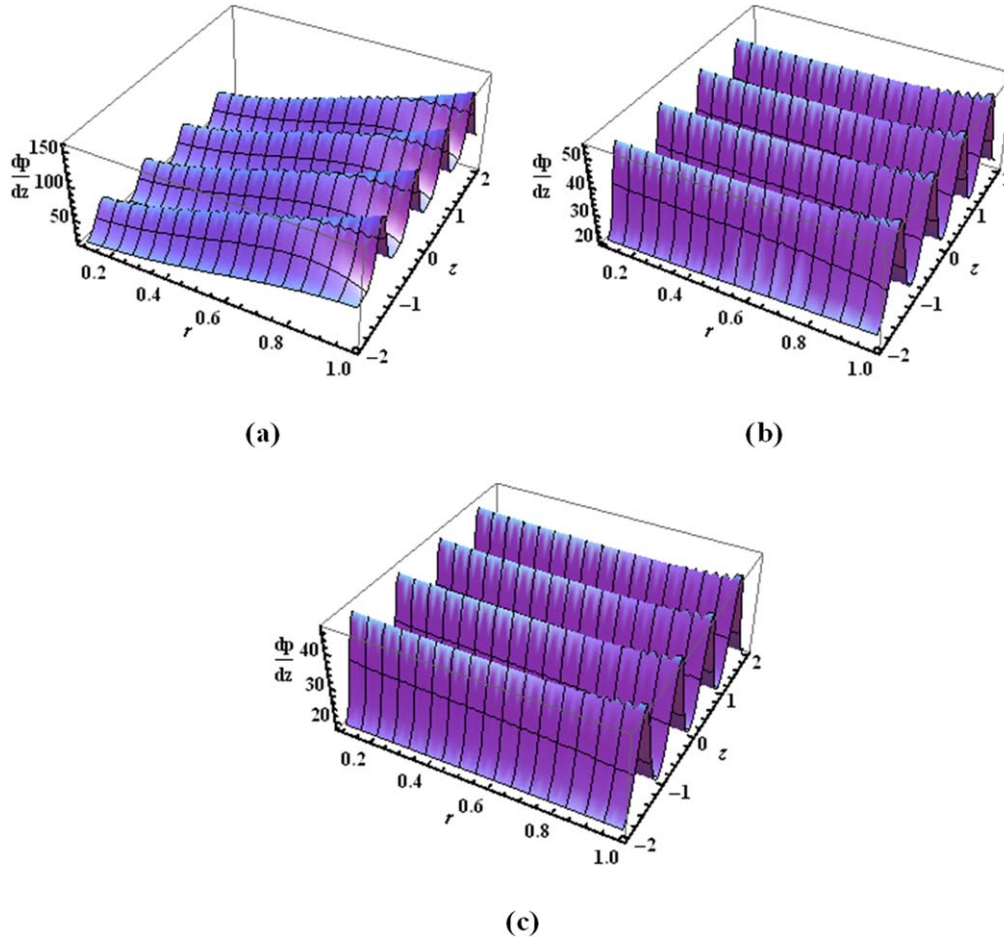
$$\frac{\partial u}{\partial r} + \frac{u}{r} = -\frac{\partial w}{\partial z}, \tag{27}$$

$$Re\beta^3\left(u\frac{\partial u}{\partial r} + w\frac{\partial u}{\partial z}\right) = -\frac{\partial p}{\partial r} + \frac{\beta}{r}\frac{\partial}{\partial r}(rS_{rr})$$

$$+ \beta^2\frac{\partial S_{zr}}{\partial z} - \beta\frac{S_{\theta\theta}}{r} - \frac{\beta}{D_a}u, \tag{28}$$

$$Re\beta\left[u\frac{\partial w}{\partial r} + w\frac{\partial w}{\partial z}\right] = -\frac{\partial p}{\partial z} + \frac{1}{r}\frac{\partial}{\partial r}(rS_{zr}) + \beta\frac{\partial S_{zz}}{\partial z}$$

$$-\left(M^2 + \frac{1}{D_a}\right)(w + 1), \tag{29}$$

where

$$S_{rr} + \lambda_1\beta\left[u\frac{\partial S_{rr}}{\partial r} + w\frac{\partial S_{rr}}{\partial z} - 2\frac{\partial u}{\partial r}S_{rr} - 2\beta\frac{\partial u}{\partial z}S_{zr}\right]$$

$$= 2\beta\frac{\partial u}{\partial r}, \tag{30}$$

(a)

(b)

(c)

Figure 4. (a)–(c) 3D view of pressure gradient for $D_a = 0.1,\ 1,\ 10$. When $Re = 1$, $\beta = 0.1$, $\alpha = 0.4$, $\varepsilon = 0.2$, $M = 1$, $\lambda_1 = 0.1$ and $\bar{Q} = -3$ are kept fixed.

$$S_{r\theta} + \beta\lambda_1\left(u\frac{\partial S_{r\theta}}{\partial r} + w\frac{\partial S_{r\theta}}{\partial z} - \frac{\partial u}{\partial r}S_{r\theta} - \beta\frac{\partial u}{\partial z}S_{z\theta}\right.$$
$$\left. - \frac{u}{r}S_{r\theta}\right) = 0 \tag{31}$$

$$S_{rz} + \lambda_1\left(\beta\left(u\frac{\partial S_{rz}}{\partial r} + w\frac{\partial S_{rz}}{\partial z}\right) - \beta\left(\frac{\partial w}{\partial z}S_{zr}\right.\right.$$
$$\left. + \frac{\partial u}{\partial r}S_{zr}\right) - \beta^2\frac{\partial u}{\partial z}S_{zz} - \frac{\partial w}{\partial r}S_{rr}\right) = \beta^2\frac{\partial u}{\partial z}$$
$$+ \frac{\partial w}{\partial r}, \tag{32}$$

$$S_{\theta\theta} + \lambda_1\beta\left(\left(u\frac{\partial}{\partial r} + w\frac{\partial}{\partial z}\right)S_{\theta\theta} - 2\frac{u}{r}S_{\theta\theta}\right) = 2\beta\frac{u}{r}, \tag{33}$$

$$S_{\theta z} + \lambda_1\left(\beta\left(u\frac{\partial S_{\theta z}}{\partial r} + w\frac{\partial S_{\theta z}}{\partial z}\right) - \beta\left(\frac{u}{r}S_{\theta z}\right.\right.$$
$$\left. + \frac{\partial w}{\partial z}S_{\theta z}\right) - \frac{\partial w}{\partial r}S_{r\theta}\right) = 0 \tag{34}$$

$$S_{zz} + \lambda_1\left[\beta\left(u\frac{\partial S_{zz}}{\partial r} + w\frac{\partial S_{zz}}{\partial z}\right) - 2\frac{\partial w}{\partial r}S_{rz}\right.$$
$$\left. - 2\beta\frac{\partial w}{\partial z}S_{zz}\right] = 2\beta\frac{\partial w}{\partial z}. \tag{35}$$

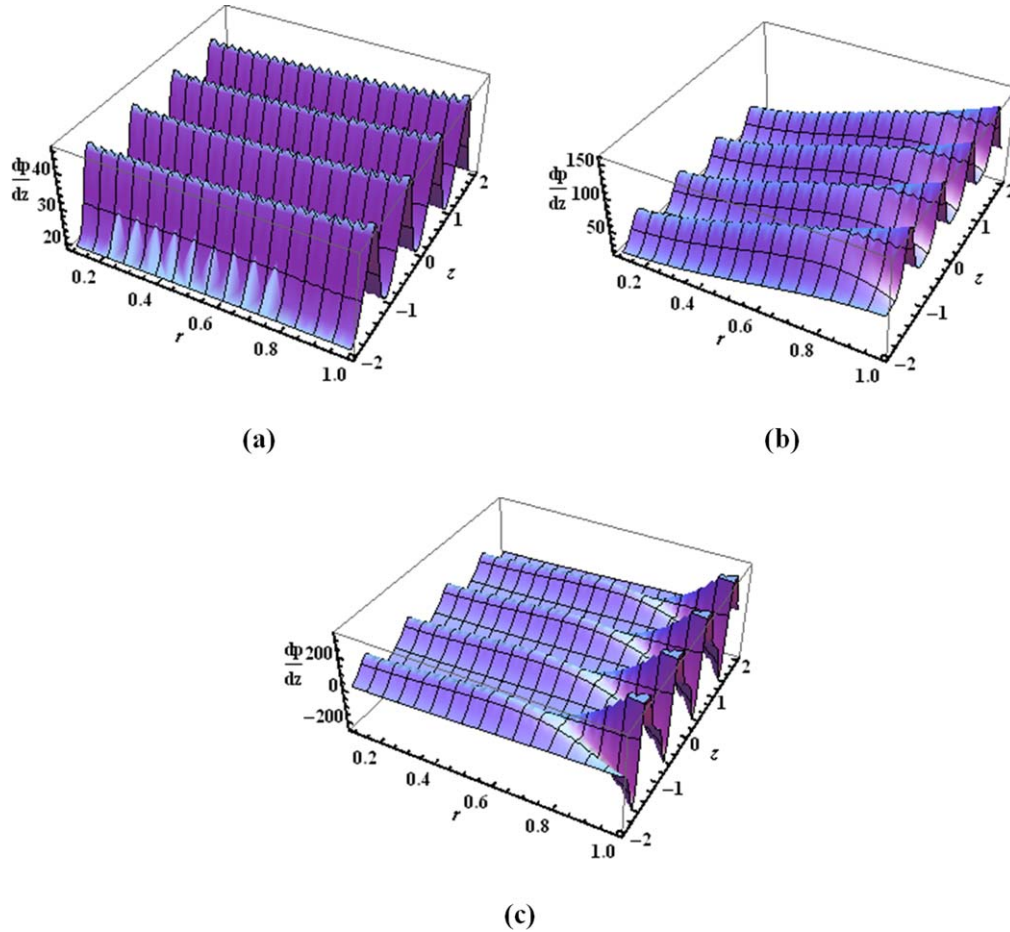The non-dimensional boundary conditions can be written as

$$w = w(h) = -(1 + 2\pi\varepsilon\alpha\beta\cos(2\pi z)), \tag{36a}$$

$$u = u(h) = \pm 2\pi\varepsilon(\sin(2\pi z))$$
$$+ \beta 2\pi\varepsilon\alpha\sin(2\pi z)\cos(2\pi z), \tag{36b}$$

at

$$r = \pm h(z) = \pm[a + \varepsilon\alpha a\cos n],$$
$$\frac{\partial w}{\partial r} = 0 \text{ at } r = 0. \tag{37}$$

Figure 5. (a)–(c) 3D view of pressure gradient for $\lambda_l = 0.1, \ 1, \ 10$. When $Re = 1$, $\beta = 0.1$, $\alpha = 0.4$, $\varepsilon = 0.2$, $M = 1$, $D_a = 1$ and $\bar{Q} = -3$ are kept fixed.

Following relations of velocity and stream function are used to simplify the equations (27)–(37)

$$u = \frac{-1}{r}\frac{\partial\psi}{\partial z}, \ w = \frac{1}{r}\frac{\partial\psi}{\partial r}. \tag{38}$$

Equation (27) is identically satisfied and equations (28)–(37) take the following form

$$Re\beta^3\left(\left(\frac{-1}{r}\frac{\partial\psi}{\partial z}\right)\frac{\partial}{\partial r}\left(-\frac{1}{r}\frac{\partial\psi}{\partial z}\right) + \left(\frac{1}{r}\frac{\partial\psi}{\partial r}\right)\frac{\partial}{\partial z}\right.$$
$$\left.\times\left(-\frac{1}{r}\frac{\partial\psi}{\partial z}\right)\right) = -\frac{\partial p}{\partial r} + \frac{\beta}{r}\frac{\partial}{\partial r}(rS_{rr}) + \beta^2\frac{\partial S_{zr}}{\partial z}$$
$$- \beta\frac{S_{\theta\theta}}{r} - \frac{\beta}{D_a}\left(-\frac{1}{r}\frac{\partial\psi}{\partial z}\right), \tag{39}$$

$$\beta Re\left(\left(\frac{-1}{r}\frac{\partial\psi}{\partial z}\right)\frac{\partial}{\partial r}\left(\frac{1}{r}\frac{\partial\psi}{\partial r}\right) + \left(\frac{1}{r}\frac{\partial\psi}{\partial r}\right)\frac{\partial}{\partial z}\right.$$
$$\left.\times\left(\frac{1}{r}\frac{\partial\psi}{\partial r}\right)\right) = -\frac{\partial p}{\partial z} + \frac{1}{r}\frac{\partial}{\partial r}(rS_{rz}) + \beta\frac{\partial S_{zz}}{\partial z}$$
$$- \left(M^2 + \frac{1}{D_a}\right)\left(\frac{1}{r}\frac{\partial\psi}{\partial r} + 1\right). \tag{40}$$

Eliminating pressure gradient from above equations, one can get the following form

$$\beta^3 Re\frac{\partial}{\partial z}\left(\frac{-1}{r}\frac{\partial\psi}{\partial z}\frac{\partial}{\partial r}\left(-\frac{1}{r}\frac{\partial\psi}{\partial z}\right) + \left(\frac{1}{r}\frac{\partial\psi}{\partial r}\right)\frac{\partial}{\partial z}\right.$$
$$\left.\times\left(-\frac{1}{r}\frac{\partial\psi}{\partial z}\right)\right) - \beta Re\frac{\partial}{\partial r}\left(\frac{-1}{r}\frac{\partial\psi}{\partial z}\frac{\partial}{\partial r}\left(\frac{1}{r}\frac{\partial\psi}{\partial r}\right)\right.$$
$$\left.+ \left(\frac{1}{r}\frac{\partial\psi}{\partial r}\right)\frac{\partial}{\partial z}\left(\frac{1}{r}\frac{\partial\psi}{\partial r}\right)\right) - \frac{\partial}{\partial r}\left(\left(M^2 + \frac{1}{D_a}\right)\right.$$
$$\left.\times\left(\frac{1}{r}\frac{\partial\psi}{\partial r} + 1\right)\right) = \frac{\partial}{\partial z}\left(\frac{\beta}{r}\frac{\partial}{\partial r}(rS_{rr}) + \beta^2\frac{\partial S_{zz}}{\partial z}\right.$$
$$\left.- \beta\frac{S_{\theta\theta}}{r}\right) - \frac{\partial}{\partial r}\left(\frac{1}{r}\frac{\partial}{\partial r}(rS_{rz}) + \beta\frac{\partial S_{zz}}{\partial z}\right), \tag{41}$$

where S_{rr}, $S_{r\theta}$, S_{rz}, $S_{\theta\theta}$, $S_{\theta z}$ and S_{zz} satisfy following equations
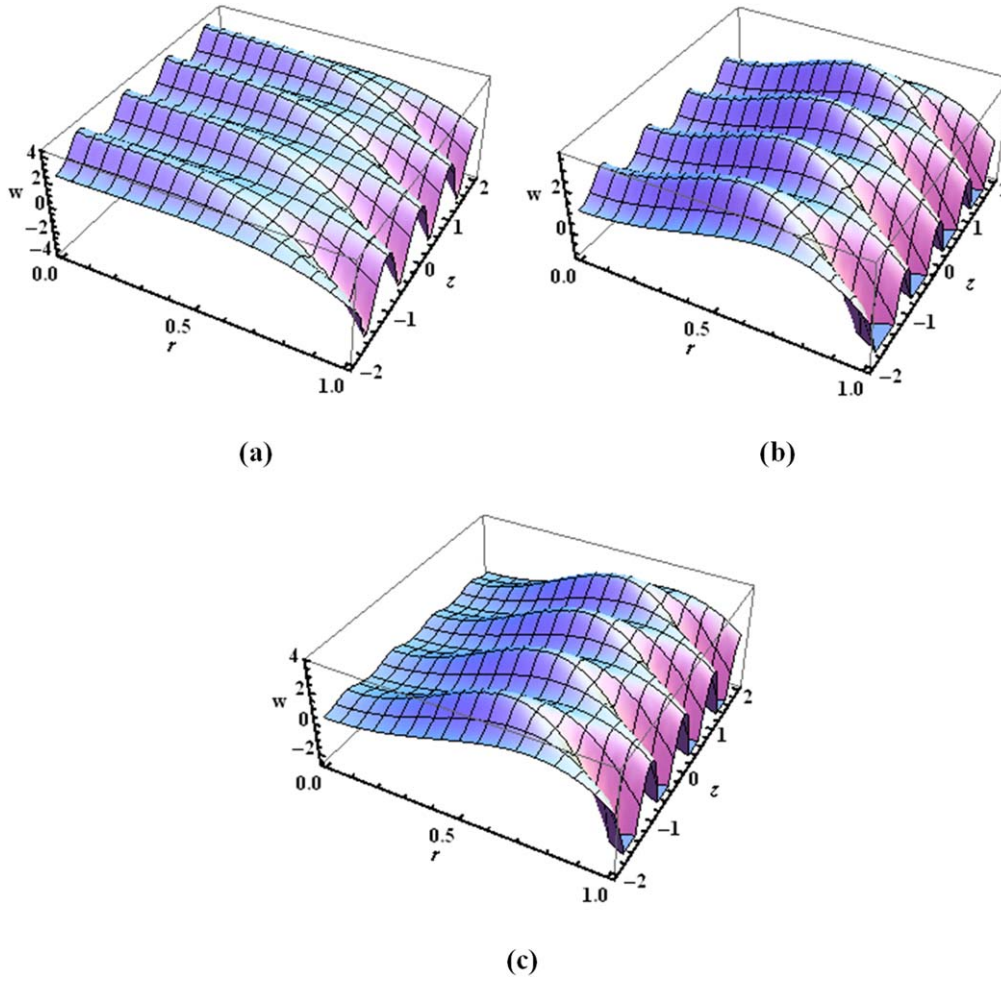
Figure 6. (a)–(c) 3D view of axial velocity for $M = 0.1, \ 1, \ 10$. With $Re = 1$, $\beta = 0.1$, $\alpha = 0.4$, $\varepsilon = 0.2$, $\lambda_1 = 1$, $D_a = 1$ and $\bar{Q} = -3$.
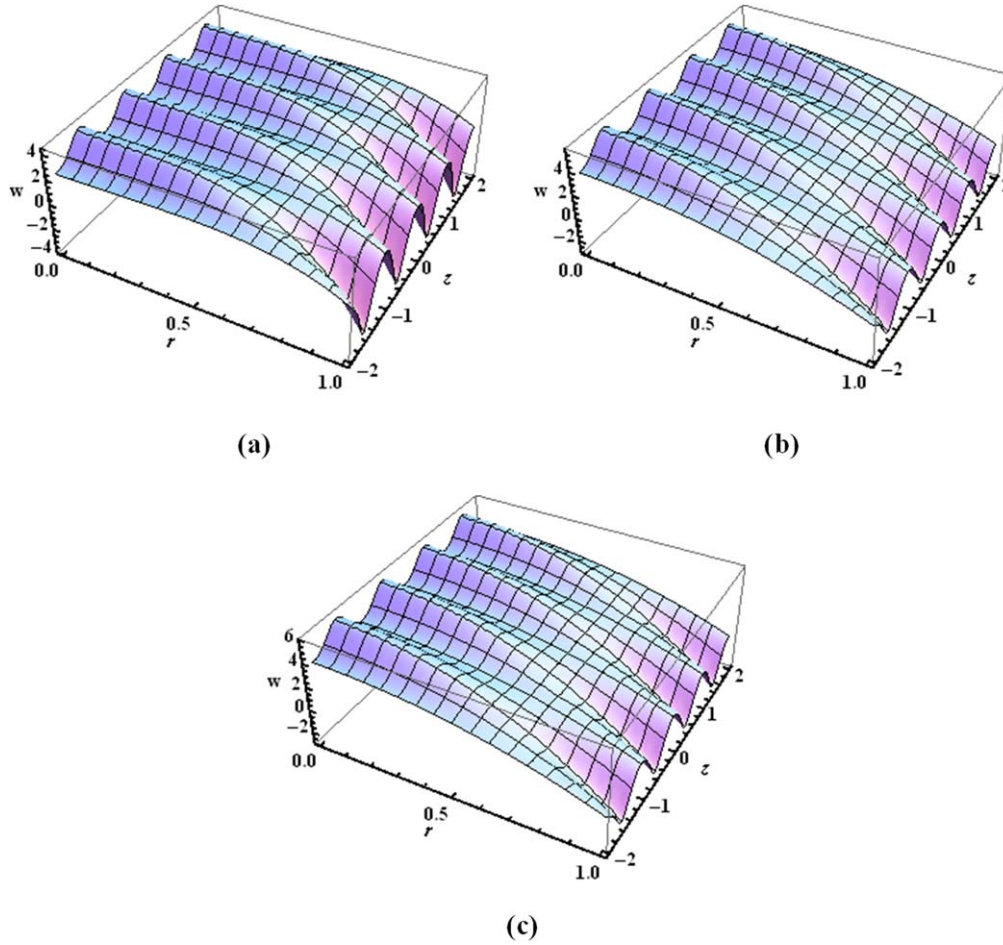
$$S_{rr} + \lambda_1 \beta \left[\frac{1}{r} \left(-\frac{\partial \psi}{\partial z} \frac{\partial S_{rr}}{\partial r} + \frac{\partial \psi}{\partial r} \frac{\partial S_{rr}}{\partial z} \right) \right.$$
$$\left. + 2\beta \frac{\partial}{\partial r} \left(\frac{1}{r} \frac{\partial \psi}{\partial z} \right) S_{rr} + 2\beta^2 \frac{\partial}{\partial z} \left(\frac{1}{r} \frac{\partial \psi}{\partial z} \right) S_{rz} \right]$$
$$= -2\beta \frac{\partial}{\partial r} \left(\frac{1}{r} \frac{\partial \psi}{\partial z} \right), \tag{42}$$

$$S_{r\theta} + \beta \lambda_1 \left(\frac{1}{r} \left(-\frac{\partial \psi}{\partial z} \frac{\partial S_{r\theta}}{\partial r} + \frac{\partial \psi}{\partial r} \frac{\partial S_{r\theta}}{\partial z} \right) \right.$$
$$+ \frac{\partial}{\partial r} \left(\frac{1}{r} \frac{\partial \psi}{\partial z} \right) S_{r\theta} + \beta \frac{\partial}{\partial z} \left(\frac{1}{r} \frac{\partial \psi}{\partial z} \right) S_{z\theta}$$
$$\left. + \frac{1}{r} \left(\frac{1}{r} \frac{\partial \psi}{\partial z} \right) S_{r\theta} \right) = 0 \tag{43}$$

$$S_{rz} + \lambda_1 \beta \left[\frac{1}{r} \left(-\frac{\partial \psi}{\partial z} \frac{\partial S_{rz}}{\partial r} + \frac{\partial \psi}{\partial r} \frac{\partial S_{rz}}{\partial z} \right) \right.$$
$$- \beta \left(\frac{\partial}{\partial z} \left(\frac{1}{r} \frac{\partial \psi}{\partial r} \right) S_{rz} - \frac{\partial}{\partial r} \left(\frac{1}{r} \frac{\partial \psi}{\partial z} \right) S_{rz} \right)$$
$$\left. + \beta^2 \frac{\partial}{\partial z} \left(\frac{1}{r} \frac{\partial \psi}{\partial z} \right) S_{zz} - \frac{\partial}{\partial r} \left(\frac{1}{r} \frac{\partial \psi}{\partial r} \right) S_{rr} \right]$$
$$= \beta^2 \frac{\partial}{\partial z} \left(\frac{-1}{r} \frac{\partial \psi}{\partial z} \right) + \frac{\partial}{\partial r} \left(\frac{1}{r} \frac{\partial \psi}{\partial r} \right), \tag{44}$$

$$S_{\theta\theta} + \lambda_1 \beta \left[\frac{1}{r} \left(-\frac{\partial \psi}{\partial z} \frac{\partial S_{\theta\theta}}{\partial r} + \frac{\partial \psi}{\partial r} \frac{\partial S_{\theta\theta}}{\partial z} \right) \right.$$
$$\left. + S_{\theta\theta} \frac{2}{r^2} \frac{\partial \psi}{\partial z} \right] = 2\beta \frac{1}{r} \left(\frac{-1}{r} \frac{\partial \psi}{\partial z} \right), \tag{45}$$

$$S_{\theta z} + \lambda_1 \left(\frac{\beta}{r} \left(\left(-\frac{1}{r} \frac{\partial \psi}{\partial z} \right) \frac{\partial S_{\theta z}}{\partial r} + \left(\frac{1}{r} \frac{\partial \psi}{\partial r} \right) \frac{\partial S_{\theta z}}{\partial z} \right) \right.$$
$$- \beta \left(\frac{-1}{r^2} \left(\frac{\partial \psi}{\partial z} \right) S_{\theta z} + \frac{\partial}{\partial z} \left(\frac{1}{r} \frac{\partial \psi}{\partial r} \right) S_{\theta z} \right)$$
$$\left. - \frac{\partial}{\partial r} \left(\frac{1}{r} \frac{\partial \psi}{\partial r} \right) S_{r\theta} \right) = 0 \tag{46}$$

8

Figure 7. (a)–(c) 3D view of axial velocity for $D_a = 0.1,\ 1,\ 10$. When $Re = 1$, $\beta = 0.1$, $\alpha = 0.4$, $\varepsilon = 0.2$, $\lambda_1 = 1$, $M = 1$ and $\bar{Q} = -3$ are kept fixed.

$$S_{zz} + \lambda_1 \left[\frac{\beta}{r} \left(-\frac{\partial \psi}{\partial z} \frac{\partial S_{zz}}{\partial r} + \frac{\partial \psi}{\partial r} \frac{\partial S_{zz}}{\partial z} \right) \right.$$
$$\left. - 2 \frac{\partial}{\partial r} \left(\frac{1}{r} \frac{\partial \psi}{\partial r} \right) S_{rz} - 2\beta \frac{\partial}{\partial z} \left(\frac{1}{r} \frac{\partial \psi}{\partial r} \right) S_{zz} \right]$$
$$= 2\beta \frac{\partial}{\partial z} \left(\frac{1}{r} \frac{\partial \psi}{\partial r} \right). \tag{47}$$

The transformed boundary conditions are defined as

$$\psi = 0 \quad \text{by convension} \tag{48a}$$

$$\frac{\partial}{\partial r} \left(\frac{1}{r} \frac{\partial \psi}{\partial r} \right) = 0 \text{ by symmetry} \quad \text{at } r = 0 \tag{48b}$$

$$\left(\frac{1}{r} \frac{\partial \psi}{\partial r} \right) = w(h) \text{ by no slip condition} \tag{48c}$$

$$\psi = 0 \quad \text{at } r = h. \tag{48d}$$

The flow rate of mucus in human bronchial tube ranges from $(0.1 - 0.6)$mm min^{-1}, therefore it is important to calculate flow rate of mucus from the airways to the ciliated epithelium. The volume flow rate in the wave and fixed frame can be calculated by the following formulas

$$Q(Z, t) = 2\pi \int_0^h RW(R, Z, t)\mathrm{d}R, \text{ (Fixed Frame)} \tag{49}$$
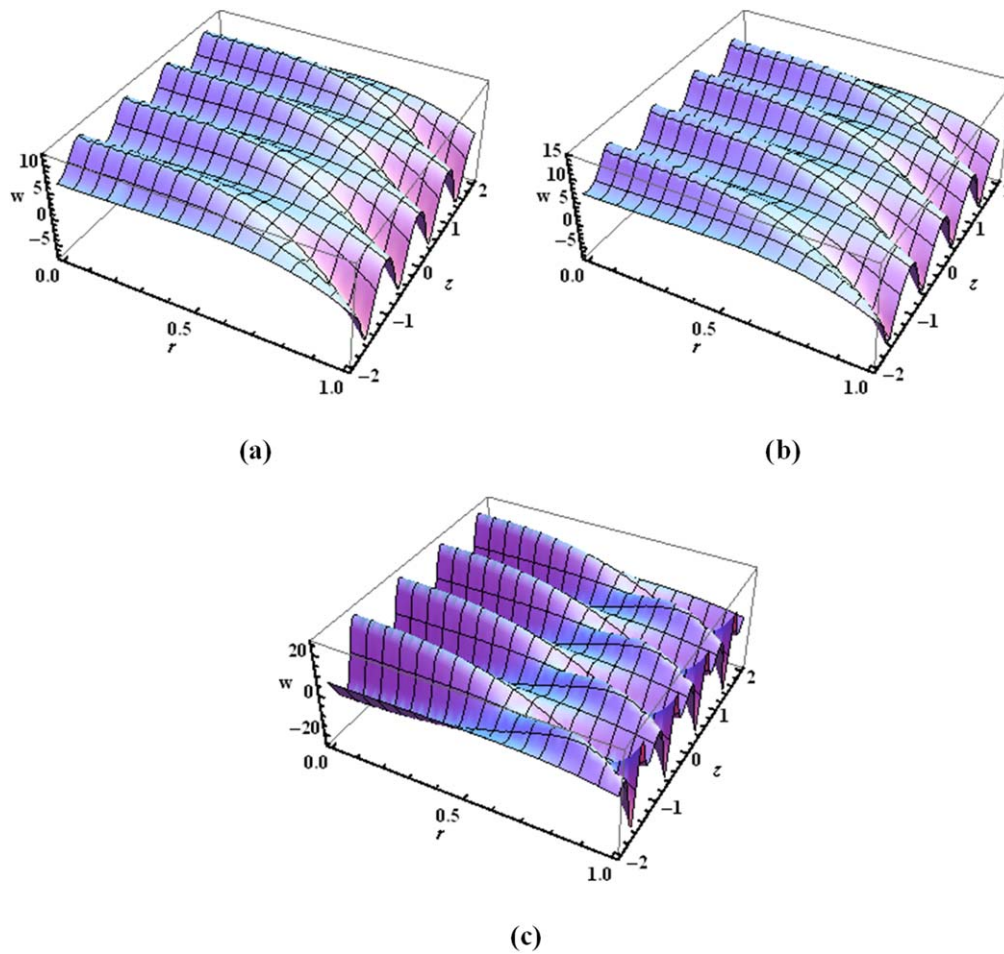
$$q = 2\pi \int_0^h rw(r, z)\mathrm{d}r, \text{ (Wave Frame)}. \tag{50}$$

Continuity and above equations yield following relation

$$Q(Z, t) = q + c\pi h^2. \tag{51}$$

The mean-time volume flow rate can be defined as follows

$$Q^* = \frac{1}{T} \int_0^1 Q\mathrm{d}t = q + a^2 c\pi \left(1 + \frac{\varepsilon^2}{2} \right). \tag{52}$$

Figure 8. (a)–(c) 3D view of axial velocity for $\lambda_1 = 0.1,\ 1,\ 10$. When $Re = 1$, $\beta = 0.1$, $\alpha = 0.4$, $\varepsilon = 0.2$, $D_a = 1$, $M = 1$ and $\bar{Q} = -3$ are kept fixed.

Defining $\bar{Q} = \frac{Q^*}{2\pi a^2 c}$ and $F = \frac{q}{2\pi a^2 c}$ we can write following relation

$$\bar{Q} = F + \left(1 + \frac{\varepsilon^2}{2}\right). \tag{53}$$

3. Perturbation solution

To find perturbation solution of proposed problem we will expand the stream function ψ, pressure distribution p, stress S and flux F in power series of small parameter $\beta \ll 1$ (Since wave number have inverse relationship with wavelength and wave length of metachronal wave is large as compared to diameter of tube) as follows

$$\psi = \psi_0 + \beta\psi_1 + \beta^2\psi_2 \dots\dots\dots \tag{54a}$$

$$p = p_0 + \beta p_1 + \beta^2 p_2 \dots\dots\dots \tag{54b}$$

$$S = S_0 + \beta S_1 + \beta^2 S_2 \dots\dots\dots \tag{54c}$$

$$F = F_0 + \beta F_1 + \beta^2 F_2 \dots\dots\dots \tag{54d}$$

3.1. Zeroth order solution

After substituting equations (54a)–(54d) in (41)–(47) and comparing the coefficients of (β^0), following boundary value problems for the stream function, pressure gradient and stress components can be obtained

$$\frac{\partial}{\partial r}\left(\frac{1}{r}\frac{\partial}{\partial r}\left(r\frac{\partial}{\partial r}\left(\frac{1}{r}\frac{\partial\psi_0}{\partial r}\right)\right)\right)$$
$$- \left(M^2 + \frac{1}{D_a}\right)\frac{\partial}{\partial r}\left(\frac{1}{r}\frac{\partial\psi_0}{\partial r}\right) = 0, \tag{55a}$$

$$\frac{\partial p_0}{\partial z} = \frac{1}{r}\frac{\partial}{\partial r}\left(r\frac{\partial}{\partial r}\left(\frac{1}{r}\frac{\partial\psi_0}{\partial r}\right)\right)$$
$$- \left(M^2 + \frac{1}{D_a}\right)\left(\frac{1}{r}\frac{\partial\psi_0}{\partial r} + 1\right), \tag{55b}$$

$$\frac{\partial p_0}{\partial r} = 0, \tag{55c}$$

$$S_{0rr} = 0, \tag{55d}$$

$$S_{0rz} = \frac{\partial}{\partial r}\left(\frac{1}{r}\frac{\partial\psi_0}{\partial r}\right), \tag{55e}$$

$$S_{0zz} = 2\lambda_1 \frac{\partial}{\partial r}\left(\frac{1}{r}\frac{\partial \psi_0}{\partial r}\right) S_{0rz} \tag{55f}$$

$$S_{0\theta\theta} = 0 \tag{55g}$$

with the boundary conditions

$$\psi_0 = 0, \ \frac{\partial}{\partial r}\left(\frac{1}{r}\frac{\partial \psi_0}{\partial r}\right) = 0 \text{ at } r = 0 \tag{56a}$$

$$\psi_0 = F_0, \frac{\partial \psi_0}{\partial r} = w(h) \text{ at } r = h. \tag{56b}$$

Integrating equation (55a) and using boundary conditions in equation (56) one can get the following integro differential equation

$$\frac{\mathrm{d}\psi_0}{\mathrm{d}r} - \left(M^2 + \frac{1}{D_a}\right)\int_0^r \left(\frac{r}{t}\right)\psi_0(t)\mathrm{d}t = c_1\frac{r^3}{4} + c_3 r. \tag{57}$$

The above Integro-differential equation is solved with the help of ADM.

Linear operator and inverse linear operator can be chosen as follows

$$\mathcal{L} = \frac{\mathrm{d}}{\mathrm{d}r}, \ \mathcal{L}^{-1} = \int_0^r (\cdot)\mathrm{d}r. \tag{58}$$

With the help of above inverse operator equation (57) takes the following form

$$\psi_0(r) = \mathcal{L}^{-1}(f(r)) \\ + \mathcal{L}^{-1}\left[\left(M^2 + \frac{1}{D_a}\right)\int_0^r K(r,t)\psi_0(t)\mathrm{d}t\right], \tag{59}$$

where

$$f(r) = c_1\frac{r^3}{4} + c_3 r, \ K(r,t) = \frac{r}{t}. \tag{60}$$

ADM suggest the following series

$$\psi_0 = \sum_{n=0}^{\infty} \psi_{0n}. \tag{61}$$

Using above equation in equation (59) following recursive relation is obtained

$$\psi_{00}(r) = \mathcal{L}^{-1}(f(r)), \tag{62}$$

$$\psi_{0(n+1)}(r) = \mathcal{L}^{-1}\left[\left(M^2 + \frac{1}{D_a}\right)\int_0^r K(r,t)\psi_{0n}(t)\mathrm{d}t\right], \\ n > 0. \tag{63}$$

Using equations (57) and (63) following equations can be evaluated

$$\psi_0 = \psi_{00} + \psi_{01} + \psi_{02} + \cdots\cdots, \tag{64}$$

$$\psi_0 = c_1\left(\frac{r^4}{16} + \frac{r^6\left(M^2 + \frac{1}{D_a}\right)^2}{384}\right) \\ + c_3\left(\frac{r^2}{2} + \frac{r^4\left(M^2 + \frac{1}{D_a}\right)^2}{16}\right) + \cdots\cdots \tag{65}$$

Making use of boundary conditions given in equations (56a), (56b) we arrive at zeroth order solution

$$\psi_0 = A_1 r^2 + A_2 r^4 + A_3 r^6. \tag{66}$$

Substituting equation (66) and equations (55d)–(55g) in equation (56b) we can get $\frac{\partial p_0}{\partial z}$ which is calculated by using software 'MATHEMATICA' as

$$\frac{\partial p_0}{\partial z} = A_4 + A_5 r^2 + A_6 r^4, \tag{67}$$

where $A_I(M, D_a, h, w(h))(1 \leqslant i \leqslant 5)$ are evaluated by 'MATHEMATICA'

$$\frac{\partial p_0}{\partial r} = 0. \tag{68}$$

3.2. First order solution

We can write the following first order problem in the analogy of equations (56) and (57)

$$Re\frac{\partial}{\partial r}\left(-\frac{1}{r}\frac{\partial \psi_0}{\partial z}\frac{\partial}{\partial r}\left(\frac{1}{r}\frac{\partial \psi_0}{\partial r}\right) + \left(\frac{1}{r}\frac{\partial \psi_0}{\partial r}\right)\frac{\partial}{\partial z}\right. \\ \left. \times \left(\frac{1}{r}\frac{\partial \psi_0}{\partial z}\right)\right) - \left(M^2 + \frac{1}{D_a}\right)\frac{\partial}{\partial r}\left(\frac{1}{r}\frac{\partial \psi_1}{\partial r}\right) \\ = \frac{\partial}{\partial z}\left(\frac{1}{r}\frac{\partial}{\partial r}(rS_{0rr}) - \frac{S_{0\theta\theta}}{r}\right) \\ - \frac{\partial}{\partial r}\left(\frac{1}{r}\frac{\partial}{\partial r}(rS_{1rz}) + \frac{\partial S_{0zz}}{\partial z}\right) \tag{69a}$$

$$\frac{\partial p_1}{\partial z} = -Re\left(\left(\frac{-1}{r}\frac{\partial \psi_0}{\partial z}\right)\frac{\partial}{\partial r}\left(\frac{1}{r}\frac{\partial \psi_0}{\partial r}\right)\right. \\ \left. + \left(\frac{1}{r}\frac{\partial \psi_0}{\partial r}\right)\frac{\partial}{\partial z}\left(\frac{1}{r}\frac{\partial \psi_0}{\partial r}\right)\right) + \frac{1}{r}\frac{\partial}{\partial r}(rS_{1rz}) \\ + \frac{\partial S_{0zz}}{\partial z}\left(M^2 + \frac{1}{D_a}\right)\left(\frac{1}{r}\frac{\partial \psi_0}{\partial r} + 1\right) \tag{69b}$$

$$\frac{\partial p_1}{\partial r} = 0, \tag{69c}$$

$$S_{1rr} = -2\frac{\partial}{\partial r}\left(\frac{1}{r}\frac{\partial \psi_0}{\partial z}\right), \tag{69d}$$

$$S_{1rz} = \frac{\partial}{\partial r}\left(\frac{1}{r}\frac{\partial \psi_1}{\partial z}\right)$$

$$- \lambda_1\left[\left(-\frac{1}{r}\frac{\partial \psi_0}{\partial z}\frac{\partial}{\partial r} + \frac{1}{r}\frac{\partial \psi_0}{\partial r}\frac{\partial}{\partial z}\right)\right]S_{0rz}$$

$$- S_{1rr}\frac{\partial}{\partial r}\left(\frac{1}{r}\frac{\partial \psi_0}{\partial r}\right) - \left[\frac{\partial}{\partial r}\left(\frac{1}{r}\frac{\partial \psi_0}{\partial z}\right)\right.$$

$$\left. + \frac{\partial}{\partial z}\left(\frac{1}{r}\frac{\partial \psi_0}{\partial r}\right)\right]S_{0rz} \qquad (69e)$$

and the boundary conditions are

$$\psi_1 = 0, \ \frac{\partial}{\partial r}\left(\frac{1}{r}\frac{\partial \psi_1}{\partial r}\right) = 0 \text{ at } r = 0. \qquad (70)$$

Following the same procedure of zeroth order system one can get following equation

$$\frac{d\psi_1}{dr} - \left(M^2 + \frac{1}{D_a}\right)\int_0^r \left(\frac{r}{t}\right)\psi_1(t)dt = A_7\frac{r^5}{45}$$

$$+ A_8\frac{r^6}{48 * 6} + A_9\frac{r^7}{7 * 75} + A_{10}\frac{r^7}{7 * 75}$$

$$+ A_{10}\frac{r^8}{8 * 144} + A_{11}\frac{r^9}{7 * 9 * 35} + A_{12}\frac{r^{10}}{8 * 10 * 48}$$

$$+ A_{13}\frac{r^{11}}{9 * 11 * 63} + A_{14}\frac{r^{12}}{10 * 12 * 80} + c_5\frac{r^4}{16}$$

$$+ c_7\frac{r^2}{2}. \qquad (71)$$

The above equation is integro-differential equation which is solved by applying ADM.

Applying $\mathcal{L}^{-1}$ on equation (71) one can get

$$\psi_1(r) = \mathcal{L}^{-1}(f(r))$$

$$+ \mathcal{L}^{-1}\left[\left(M^2 + \frac{1}{D_a}\right)\int_0^r K(r, t)\psi_1(t)dt\right], \qquad (72)$$

where

$$f(r) = A_7\frac{r^5}{45} + A_8\frac{r^6}{48 * 6} + A_9\frac{r^7}{7 * 75} + A_{10}\frac{r^7}{7 * 75}$$

$$+ A_{10}\frac{r^8}{8 * 144} + A_{11}\frac{r^9}{7 * 9 * 35} + A_{12}\frac{r^{10}}{8 * 10 * 48}$$

$$+ A_{13}\frac{r^{11}}{9 * 11 * 63} + A_{14}\frac{r^{12}}{10 * 12 * 80} + c_5\frac{r^4}{16}$$

$$+ c_7\frac{r^2}{2} \qquad (73)$$

ψ_1 can be decomposed into the following series

$$\psi_1 = \sum_{n=0}^{\infty} \psi_{1n}. \qquad (74)$$

Initial guess is chosen as follows

$$\psi_{10}(r) = \mathcal{L}^{-1}(f(r)), \qquad (75)$$

$$\psi_{1(n+1)}(r) = \mathcal{L}^{-1}\left[\left(M^2 + \frac{1}{D_a}\right)\int_0^r K(r, t)\psi_{1n}(t)dt\right],$$

$$n > 0.$$

$$(76)$$

Using equations (75)–(76) in (74) we can get ψ_1 in the following form

$$\psi_1 = c_4\left(\frac{r^4}{16} + \frac{r^6N^2}{384}\right) + c_5\left(\frac{r^2}{2} + \frac{r^4N^2}{16}\right)$$

$$+ A_7\left(\frac{r^5}{45} + \frac{r^7N^2}{1575}\right) + A_8\left(\frac{r^6}{48 * 6} + \frac{r^8N^2}{13824}\right)$$

$$+ A_9\left(\frac{r^7}{75 * 7} + \frac{r^9N^2}{33705}\right) + A_{10}\left(\frac{r^8}{8 * 144} + \frac{r^{10}N^2}{92160}\right)$$

$$+ A_{11}\left(\frac{r^9}{7 * 9 * 35} + \frac{r^{11}N^2}{218295}\right) + A_{12}\left(\frac{r^{10}}{48 * 8 * 10}\right.$$

$$+ \left.\frac{r^{12}N^2}{460800}\right) + A_{13}\left(\frac{r^{11}}{11 * 9 * 63} + \frac{r^{13}N^2}{891891}\right)$$

$$+ A_{14}\left(\frac{r^{12}}{80 * 10 * 12} + \frac{r^{14}N^2}{1612800}\right). \qquad (77)$$

Using boundary conditions given in equation (70) we arrived at first order solution

$$\psi_1 = A_{15}r^2 + A_{16}r^4 + A_{17}r^5 + A_{18}r^6 + A_{19}r^7$$

$$+ A_{20}r^8 + A_{21}r^9 + A_{22}r^{10} + A_{23}r^{11}$$

$$+ A_{24}r^{12} + A_{25}r^{13} + A_{26}r^{14}. \qquad (78)$$

Substituting equations (78) and (69c)–(69e) in (69b) we get $\frac{\partial p_1}{\partial z}$ which is calculated by using software 'MATHEMATICA' as

$$\frac{\partial p_1}{\partial z} = A_{27} + A_{28}r + A_{29}r^2 + A_{30}r^3 + A_{31}r^4$$

$$+ A_{32}r^5 + A_{33}r^6 + A_{34}r^7 + A_{35}r^8 + A_{36}r^9$$

$$+ A_{37}r^{10} + A_{38}r^{11} + A_{39}r^{12}, \qquad (79)$$

where $A_I(M, D_a, h, w(h), \lambda_1)(15 \leqslant i \leqslant 39)$ are evaluated by 'MATHEMATICA'

$$\frac{\partial p_1}{\partial r} = 0. \qquad (80)$$

4. Graphical results

In this section the effects of emerging parameters appearing in the magnetically actuated mucociliary pumping are shown

graphically. The effect of viscoelastic parameter λ_l, Hartmann number M and Darcy's parameter D_a, are observed on the pressure rise, pressure gradient and axial velocity.

Effect of emerging parameter on pressure difference are displayed by the bar charts through figures 2(a)–(c). Figure 2(a) shows that by increasing relaxation time λ_l, pressure difference enhances. The increasing value of relaxation time λ_l demonstrates that decay in stress requires more time and also it measures the viscosity of viscoelastic material. The increasing value of λ_l means that viscosity of viscoelastic material increases which requires high pressure to flow in the continuum regime. Figure 2(b) shows that by increasing Hartmann number M pressure rise increases because Lorentz force is acting in the perpendicular direction of the flow which resists the fluid motion, for the mucociliary movement through bronchial tube more change in the pressure is required with the increasing value of constant magnetic field parameter. Figure 2(*c*) shows that by increasing Darcy's parameter D_a pressure rise decreases because when Darcy's number increases the volume fraction ratio increases which permits the fluid to flow with less amount of pressure.

3D plots of pressure gradient for various values of, viscoelastic parameter λ_l, Hartmann number M and Darcy's parameter D_a are plotted in figures 3–5 It is observed that pressure gradient form a wavy pattern because fluid particles trace the shape of metachronal wave. In figures 3(a)–(c) it is shown that by increasing Hartmann number M the amplitude of elliptic wave increases as Hartmann number is the ratio of Lorentz force to viscous force, therefore increase in Hartmann number shows that Lorentz force is dominant over the viscous forces and Lorentz force has the ability to resist the fluid flow which requires large amount of pressure to maintain the same flux. It is depicted from figures 4(a)–(c) that by increasing Darcy's parameter amplitude of pressure gradient decreases because Darcy's number is the ratio of pore volume to the bulk volume which is mostly less than one, if we increase the porosity parameter more fluid flows from pores with low pressure gradient. Figures 5(a)–(c) illustrates that by increasing viscoelastic parameter λ_l amplitude of wave increases because by increasing viscoelastic parameter elastic forces begin to dominant over the viscous forces and the mucus requires large amount of pressure to return in relaxed state after deformation.

Figures 6–8 display 3D view of axial component of velocity for distinct values of viscoelastic parameter λ_l, Hartmann number M and Darcy's parameter D_a. It is observed that fluid particles follow the wave pattern due to formation of metachronal waves at the boundary. In figures 6(a)–(c) it is shown that by increasing Hartmann number M amplitude of wave decreases, as magnetic force opposes fluid flow that results to decrease in the magnitude of velocity profile. Figures 7(a)–(c) shows that with the increasing value of Darcy's parameter, magnitude of the velocity (in the wave form) increases because increasing value of Darcy's parameter indicate that pore volume increases which permits the fluid to flow through the axisymmetric tube (continuum regime). Since the pore volume assists the fluid flow, therefore velocity profile in wave form increases with the

increasing values of porosity parameter. Figures 8(a)–(c) portrays that waving velocity of mucus layer decreases with the increasing value of relaxation time λ_l, because the increasing values of λ_l indicate that viscosity of viscoelastic fluid (mucus layer) increases which causes to slow the movement of mucus, therefore axial velocity reduces with the increasing value of λ_l.

5. Conclusions

In this research we have modelled the boundary value problem of magnetically actuated mucociliary pumping in bronchial tube. For the mucociliary pumping we have considered the mathematical model of magnetically actuated muco ciliary pumping in bronchial tube with the Darcy's law in the presence of constant magnetic field. Perturbation solution of the problem is obtained using small wave number $\beta \ll 1$. If $Re \rightarrow 0$, $\lambda_l \rightarrow 0$ and $D_a \rightarrow 0$ the present model reduces to the viscous model and our results are matching precisely with the existing results [23]. The results obtained by the ADM and perturbation method are convergent because the resulting expressions of stream function and pressure gradient are in the form of power series with decaying coefficients in the given domain. The graphs of pressure rise with volume flow rate, pressure gradient and velocity field are plotted for different values of prominent parameters. From graphs the noteworthy results are as follows:

- Volume flow rate and pressure rise show a reverse behavior against all important parameters e.g., Maxwell's parameter, Hartmann number and Darcy's number.
- It is found that the pumping due to ciliary activity has to work more efficiently for pushing the MHD fluid if compared with a simple Newtonian fluid.
- It is observed that in highly porous medium magnetically actuated cilia are very helpful to clear thin layer of mucus.
- It is investigated that the velocity of fluid decays with the increase in relaxation time (viscoelastic parameter) which make the mucus thick.
- The obtained results are useful in transport phenomena of physiological systems i.e., if the fluid becomes thick due to infection and congestion of throat the mucus cannot flow freely. This study shows that mucus become thin by the application of magnetic field in the direction of flow field and mucus layer become thick if magnetic field is applied in the transverse direction of the flow field.
- The present study is applicable in oesophageal transport, bio fluid mechanics and other areas of physiology.
- In this study we have considered the single layer of mucus in the bronchial tube with the effects of constant magnetic field and porous medium but the mucus near the epithelium cell and near the center of the bronchial tube have different viscosity, so we will consider the two layer approach of ciliary motion in the future work.

ORCID iDs

K Maqbool ⓘ https://orcid.org/0000-0002-3822-593X

References

[1] Elnaqeeb T, Mekheimer K S and Alghamdi F 2016 Cu-blood flow model through a catheterized mild stenotic artery with a thrombosis *Math. Biosci.* **282** 135–46

[2] Elnaqeeb T, Shah N A and Mekheimer K S 2019 Hemodynamic characteristics of gold nanoparticle blood flow through a tapered stenosed vessel with variable nanofluid viscosity *BioNanoScience* **9** 245–55

[3] Sleigh M A, Blake J R and Liron N 1988 The propulsion of mucus by cilia *Am. Rev. Respiratory Dis.* **137** 726–41

[4] Lindemann C B and Lesich K A 2010 Flagellar and ciliary beating: the proven and the possible *J. Cell Sci.* **123** 519–28

[5] Ibañez-Tallon I, Heintz N and Omran H 2003 To beat or not to beat: roles of cilia in development and disease *Hum. Mol. Genet.* **12** R27–35

[6] Brennen C and Winet H 1977 Fluid mechanics of propulsion by cilia and flagella *Annu. Rev. Fluid Mech.* **9** 339–98

[7] Verdugo P 1982 Introduction: mucociliary function in mammalian epithelia *Cell Motil.* **2** 1–5

[8] Blake J 1975 On the movement of mucus in the lung *J. Biomech.* **8** 179–90

[9] Sanderson M J and Sleigh M A 1981 Ciliary activity of cultured rabbit tracheal epithelium: beat pattern and metachrony *J. Cell Sci.* **47** 331–477263784

[10] Ross S M and Corrsin S 1974 Results of an analytical model of mucociliary pumping *J. Appl. Physiol.* **37** 333–40

[11] Mercke U 1975 The influence of varying air humidity on mucociliary activity *Acta oto-laryngologica* **79** 133–9

[12] Farooq A A, Tripathi D and Elnaqeeb T 2019 On the propulsion of micropolar fluid inside a channel due to ciliary induced metachronal wave *Appl. Math. Comput.* **347** 225–35

[13] Dauptain A, Favier J and Bottaro A 2008 Hydrodynamics of ciliary propulsion *J. Fluids Struct.* **24** 1156–65

[14] Guo H, Nawroth J, Ding Y and Kanso E 2014 Cilia beating patterns are not hydrodynamically optimal *Phys. Fluids* **26** 091901

[15] Khaderi S N, Den Toonder J M J and Onck P R 2012 Magnetically actuated artificial cilia: the effect of fluid inertia *Langmuir* **28** 7921–37

[16] Akbar N S, Tripathi D, Khan Z H and Bég O A 2017 Mathematical model for ciliary-induced transport in MHD flow of Cu–H_2O nanofluids with magnetic induction *Chin. J. Phys.* **55** 947–62

[17] Abdelsalam S, Bhatti M M, Zeeshan A, Riaz A and Beg O A 2019 Metachronal propulsion of a magnetized particle-fluid suspension in a ciliated channel with heat and mass transfer *Phys. Scr.* **94** PHYSSCR-108009.R1

[18] Abbasi F M, Shanakhat I and Shehzad S A 2019 Analysis of entropy generation in peristaltic nanofluid flow with Ohmic heating and Hall current *Phys. Scr.* **94** 025001

[19] Hassan M A 2019 Slow motion of a slip spherical particle through a viscoelastic Giesekus fluid in a peristaltic tube *Phys. Scr.* **94** 105011

[20] Vélez-Cordero J R and Lauga E 2013 Waving transport and propulsion in a generalized Newtonian fluid *J. Non-Newton. Fluid Mech.* **199** 37–50

[21] Bottier M, Fernández M P, Pelle G, Isabey D, Louis B, Grotberg J B and Filoche M 2017 A new index for characterizing micro-bead motion in a flow induced by ciliary beating: II. Modeling *PLoS Comput. Biol.* **13** e1005552

[22] Abbasi A, Ahmad I, Ali N and Hayat T 2016 An analysis of peristaltic motion of compressible convected Maxwell fluid *AIP Adv.* **6** 015119

[23] Siddiqui A M, Farooq A A and Rana M A 2014 Hydromagnetic flow of Newtonian fluid due to ciliary motion in a channel *Magnetohydrodynamics* **50** 109–22